

Artificial ASMR: A Cyber-Psychological Study

Zexin Fang*, Bin Han*, C. Clark Cao[†], and Hans D. Schotten*[‡]

*Technische Universität Kaiserslautern, [†]Lingnan University, [‡]German Research Center of Artificial Intelligence (DFKI)

Abstract—The popularity of Autonomous Sensory Meridian Response (ASMR) has skyrocketed over the past decade, but scientific studies on it are still few and immature. With our attention caught by the common acoustic patterns in ASMR audios, we investigate the correlation between the time-frequency and cyclic features of audio signals and their effectiveness in triggering ASMR effects. A cyber-psychological approach that combines signal processing, artificial intelligence, and experimental psychology is taken, with which we are able to identify ASMR-related acoustic features, and therewith synthesize random artificial ASMR audios.

Index Terms—ASMR, auditory, cyclostationary, GAN

I. INTRODUCTION

Autonomous Sensory Meridian Response (ASMR), a term that was coined in the 2010s, is widely used to describe an intriguing phenomenon in which specific visual and auditory stimuli trigger tingling sensations accompanied by positive emotions as well as a feeling of deep relaxation [1]. Common auditory triggers of ASMR include repetitive soft sounds such like finger tapping, scratching, chewing, or whispering.

With its blooming cultural popularity and growing commercial market [2], ASMR has attracted emerging research interests [3], and its cognitive effect has been verified by significant behavioral and neurological evidences [4], [5]. However, to the best of our knowledge, existing work have only identified some semantic elements that trigger the ASMR effects [6], while the acoustic features of auditory triggers remain poorly understood. Though a generic claim that low frequency sounds are widely observed from effectively triggering ASMR audios, it is not capturing the repetitive characteristic.

Inspired by an interesting study that reveals the correlation between the trypophobia-triggering effect and cyclostationary features of images [7], we suspect that the time-frequency and cyclic features of audios may also play an important role in the triggering of ASMR experience. In this paper, we prove this correlation in a cyber-psychological approach that combines various techniques of signal processing, artificial intelligence, and experimental psychology. More specifically, we apply short-time Fourier transform (STFT) and cyclic spectral analysis on recorded ASMR audio clips to extract their acoustic features. Training generative adversarial networks (GANs) in a feature-targeted manner, we are able to synthesize

This study was partly supported by the European Commission (H2020 project *Hexa-X*, GA no. 101015956), the TU Nachwuchsring at TU Kaiserslautern (individual research project *A-SIREN*), and the Lam Woo Research Fund at Lingnan University (F871223). B. Han (bin.han@eit.uni-kl.de) is the corresponding author.

artificial ASMR audio without a natural sound source. We also design a psychological survey to evaluate the effectiveness of both the recorded and synthesized ASMR audios in triggering ASMR effect on humans, and verify the correlation between this effectiveness and the selected acoustic features.

II. AUDIO DATA PROVISIONING

As the object of our study, off-the-shelf ASMR audios were obtained from non-commercial online open sources. We collected four audios recorded from real sounds of different natures, including: *i*) breathing, *ii*) mixing soft cream, *iii*) puffing a spray, and *iv*) clicking a keyboard. Every audio was recorded 16 bit stereo at the sampling rate of 22.05 kSPS, lasting about 1 h.

We intentionally select these four sound types as our experiment objects because they are largely emotionally neutral. Indeed, other common types of available ASMR audios, such like whispers, campfires, winds, chewing sounds, ocean waves, etc. usually deliver rich semantic information in their associated imagery, which may cause ASMR-independent emotional effects, and therewith generate biases in the psychological test that we are introducing in Sec. V.

III. ASMR AUDIO ANALYSIS AND FEATURE EXTRACTION

Taking a 10 s clip from the puffing spray audio and sliding a 0.1 s raised cosine window over it with 50% overlap, we can obtain an example spectrogram as shown in Fig. 1, which exhibits a general low-pass characteristic with a cyclic pattern of wide-banded bursts. Similar features were also observed in other ASMR audios we collected.

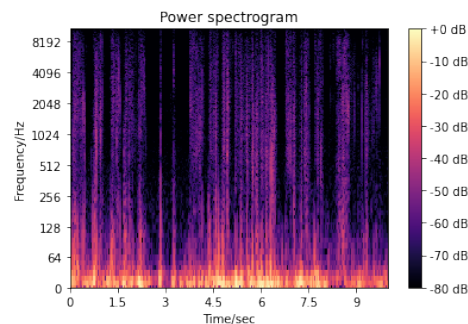


Fig. 1: Spectrogram of a puffing spray audio clip

To further investigate the periodic patterns within the PSD of x , the spectral correlation density (SCD) and cyclic coherence function (CCF) can be applied as suggested by [8]:

$$S_{XX}(f, \alpha) = \mathbb{E} \left\{ X\left(f + \frac{\alpha}{2}\right) X^*\left(f - \frac{\alpha}{2}\right) \right\} \quad (1)$$

$$C_{XX}(f, \alpha) = \frac{S_{XX}(f, \alpha)}{\sqrt{\mathbb{E} \left\{ |X\left(f + \frac{\alpha}{2}\right)|^2 \right\} \mathbb{E} \left\{ |X\left(f - \frac{\alpha}{2}\right)|^2 \right\}}} \quad (2)$$

where α is the so-called cyclic frequency that indicates the periodicity within the spectrum, and $X(f)$ the complex-valued spectrum of x at frequency f . For an N -sample signal frame x , X can be estimated by the Discrete Fourier Transform (DFT):

$$X(f) = \frac{1}{N} \sum_{k=0}^{N-1} \left[\sum_{n=0}^{N-1} x(n) e^{-j2\pi nk} \delta \left(2\pi f - \frac{2\pi k}{N} \right) \right]. \quad (3)$$

The SCD and CCF of the aforementioned spray puffing sound clip, for example, are illustrated in Fig. 2. From the figures we see a distinguishing feature that is also observed from other ASMR audios: narrow vertical stripes that distribute smoothly over a wide range in the f domain, while being discrete and sparse in the α domain, occurring at only low cyclic frequencies.

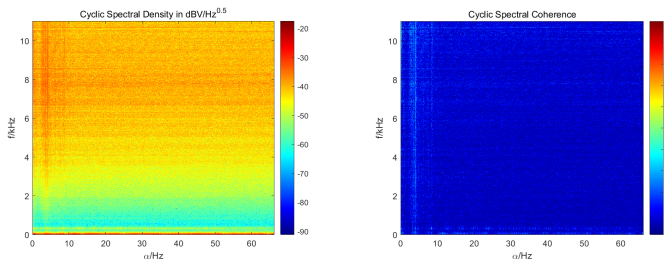


Fig. 2: SCD (left) and CCF (right) of the spray audio clip

While both SCD and CCF are bivariate functions, we further define two univariate functions of α to characterize the cyclic behavior of an audio signal x , namely $\bar{S}_{XX}(\alpha) = \frac{1}{N} \sum_{f \in \mathbb{F}} S_{XX}(f, \alpha)$ and $S_{XX}^{\max}(\alpha) = \max_{f \in \mathbb{F}} S_{XX}(f, \alpha)$, where \mathbb{F} is the set of N frequency pins in S_{XX} . \bar{S}_{XX} is sensitive to wide-banded cyclic patterns in x , while S_{XX}^{\max} is more sensitive to narrow-banded cyclic components, as illustrated in Fig. 3.

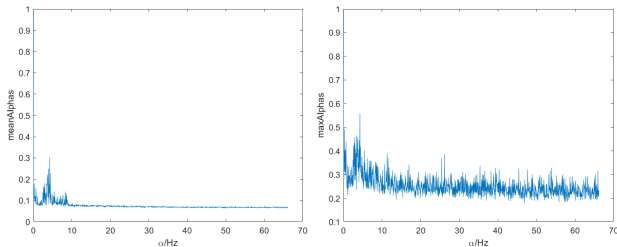


Fig. 3: \bar{S} (left) and S^{\max} (right) of the spray audio clip

On top of $X(f)$, $\bar{S}_{XX}(\alpha)$ and $S_{XX}^{\max}(\alpha)$, we define eight features: $\Phi_1(x) = \text{Mean}(\bar{S}_{XX})$, $\Phi_2(x) = \text{Var}(\bar{S}_{XX})$,

$\Phi_3(x) = G(\bar{S}_{XX})$, $\Phi_4(x) = \text{Mean}(S_{XX}^{\max})$, $\Phi_5(x) = \text{Var}(S_{XX}^{\max})$, $\Phi_6(x) = G(S_{XX}^{\max})$, $\Phi_7(x) = \text{Var}(|X|)$, and $\Phi_8(x) = G(|X|)$, where $G(\mathbb{S}) = \frac{\sum_{i \in \mathbb{S}} \sum_{j \in \mathbb{S}} |i-j|}{2\|\mathbb{S}\|_0 \sum_{i \in \mathbb{S}} i}$ is the Gini coefficient of set \mathbb{S} . Here, Φ_1 and Φ_4 assess the overall cyclostationarity, Φ_2 and Φ_5 assess the variance of cyclostationarity across different cyclic frequencies, Φ_3 and Φ_6 reflect the α -sparsity of cyclic components, Φ_7 describes the frequency-variance of SPD, and Φ_8 the frequency sparsity of SPD.

We sampled three 10 s clips from each recorded audio mentioned in Sec. II, and extracted the features Φ_1 – Φ_8 of every clip. A 10 s stereo 22.05 kSPS sampled white noise was also analyzed as benchmark. The results are listed in Tab. I.

IV. DCGAN-BASED RANDOM ASMR AUDIO SYNTHESIS

GANs, since its proposal in 2014 [9], has rapidly demonstrated its great capability of generating artificial data with certain patterns, and therewith attracted intensive attentions from research and development fields of artificial intelligence (AI). In general, a GAN system consists of two neural networks, namely the *generator* and *discriminator*, respectively. The two networks work against each other and jointly evolve, so that the generator is eventually capable of generating fake data that can be hardly distinguished from real ones [10]. Besides their iconic success in generating fake images, GANs have also been proven effective in generating/converting audio and speech signals. Several examples of recent efforts are reported in [11]–[14], which have inspired us to generate random ASMR audios with GAN.

While conventional GAN-based audio solutions are commonly specialized regarding acoustic features of natural languages or musical instruments, they cannot be straightforwardly applied on our problem. Noticing that the spectrogram of an audio signal i) contains most of the audio information, and ii) exhibits significant 2D patterns upon cyclic audio components, we propose to indirectly synthesizing ASMR audios by generating artificial ASMR-like spectrograms with GANs. More specifically, concerning the drawbacks of original GANs such like low learning stability and incapability of training with large high-definition datasets, we invoke deep convolutional GANs (DCGANs), which integrate convolutional neural networks (CNNs) into GANs to achieve better stability and efficiency of learning [15], [16].

To efficiently train the DCGAN, we set up a training data set with the four recorded ASMR audios introduced in Sec. II. We sliced from every audio 1600 segments short segments, each with 32 400 samples that correspond to about 1.5 seconds, which is sufficient to contain a ASMR-triggering pitch according to our experience. Then we carried out 2048×2048 STFT with 50% overlap between each two windows, which generated a 1025×64 power spectrogram from every individual segment. To reduce the computational load and stabilize the training of DCGAN, we downsampled every such spectrogram to the size of 192×64 , and further divided it into three 64×64 matrices, which is the a data size proven stable to train a 3-channel DCGAN as suggested

TABLE I: Features extracted from recorded ASMR audio clips

Audio Clip	Φ_1	Φ_2	Φ_3	Φ_4	Φ_5	Φ_6	Φ_7	Φ_8
White noise	2,86E-02	7,47E-05	0,0631	8,18E-03	3,88E-05	0,0426	8,20E-03	0,5226
Breathing clip 1	1,85E-04	1,56E-08	0,2727	1,60E-06	6,61E-13	0,1190	7,51E-04	0,9588
Breathing clip 2	2,78E-04	1,74E-07	0,2948	4,78E-06	5,90E-12	0,1096	1,01E-04	0,9835
Breathing clip 3	7,76E-04	5,94E-07	0,2164	9,94E-06	3,71E-11	0,1153	9,55E-05	0,9411
Soft cream clip 1	4,59E-01	1,02E-01	0,3262	1,13E-03	6,40E-07	0,2912	3,82E-04	0,9955
Soft cream clip 2	1,55E-01	8,40E-03	0,2879	4,51E-04	6,57E-08	0,2508	9,85E-04	0,9906
Soft cream clip 3	1,08E-01	6,90E-03	0,3155	2,47E-04	3,29E-08	0,3006	2,91E-04	0,9950
Spray clip 1	1,20E-03	4,81E-07	0,2833	9,42E-05	1,48E-09	0,0950	1,38E-03	0,6393
Spray clip 2	2,76E-03	2,57E-06	0,2905	1,19E-04	2,72E-09	0,0946	3,90E-03	0,6494
Spray clip 3	1,75E-03	1,08E-06	0,3073	9,21E-05	1,12E-09	0,0982	1,27E-03	0,6092
Keyboard clip 1	1,35E-03	7,54E-07	0,2382	3,93E-05	1,51E-10	0,1091	8,20E-04	0,9110
Keyboard clip 2	1,68E-03	1,12E-06	0,2341	4,33E-05	2,29E-10	0,1226	8,58E-04	0,9314
Keyboard clip 3	1,87E-03	1,55E-06	0,2330	5,18E-05	2,97E-10	0,1117	5,04E-04	0,9352

in [17]. This row-wise downsampling was carried out in a bootstrap manner to generate 30 random $64 \times 64 \times 3$ training samples out of each original power spectrogram. Thus, we obtained 192 000 training samples in total, and clustered them into 12 groups, with each group mixing samples from different audios. In addition, compared to common images where the data values are constrained within a limited quantization range, power spectrogram data usually have a significantly higher dynamic range. To keep details at the lower end of power density, the training samples are log-normalized before linearly rescaled into the range of $[-1, 1]$.

To implement the DCGAN, we created a generator model with 4 deconvolution layers, each layer is applied with a batch normalization, a *ReLU* activation, a 2×2 stride, and a 1×1 padding. Correspondingly, we created a discriminator model with 5 convolution layers, all with the same kernel, stride size, and padding size as the generator layers have. We bound both models, initialized their weights w.r.t. a normal distribution $\mathcal{N}(0, 0.02^2)$, and applied an Adam optimizer [18] with learning rate 2×10^{-4} and $\beta_1 = 0.5$.

After initialization, we fed the generator network with Gaussian white noise to synthesize artificial samples, which were then sent to the discriminator network together with the recorded samples from a certain training sample group, with a batch size of 64. The score between $[0, 1]$ given by the discriminator is then used to update the generator coefficients in the next iteration. We executed this procedure with all 12 training sample groups. We trained the networks 6 epochs, i.e. 1500 iterations for each individual group, within which the training process was generally converging, as exemplified in Fig. 4. Upon completion of the training, a 64-batch of artificial samples were generated at the output of the generator network, each sample representing the spectrogram of a 1.5 s audio segment. From each batch, we randomly selected two such samples, and repeatedly concatenated them in a random order to generate spectrograms of longer time frame. In this approach, we obtained 12 random synthesized 10 s spectrograms. While it is straightforward to apply frequency-domain linear interpolation and the Griffin-Lim algorithm [19] to reconstruct audio waveform from these synthesized spectrograms, the output generally exhibits a bad audibility. Despite of the cyclic patterns generated as expected, the reconstructed audios are commonly non-fluent and rich in high-frequency pitches

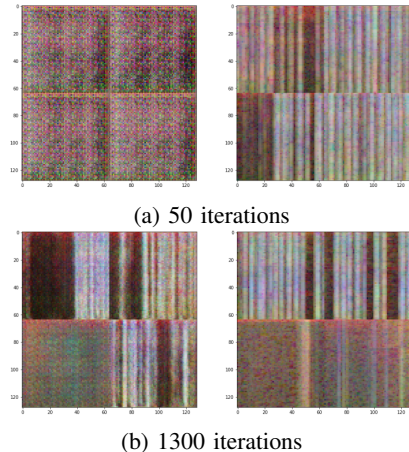


Fig. 4: Convergence of the DCGAN output: 4 synthesized (left) and 4 recorded (right) spectrogram samples

and harmonics, which make them sound harsh and piercing. These phenomena are mainly caused by the sharp transition at concatenations between different samples. To encounter such effects and improve the audibility of the synthesized ASMR, we applied moving-average smoothing on the concatenated spectrograms in both frequency and time domains, and added a weak random white noise to the power spectrogram before carrying out the audio reconstruction. These measures significantly smoothed the overall spectrum of the synthesized ASMR audios and enhanced their quality.

We extracted the same features Φ_1 – Φ_8 from the 12 audios that we reconstructed from the synthesized samples, as we did with the recorded ASMR audio clips, results are in Tab. II.

V. BEHAVIORAL STUDY OF ASMR TRIGGERING EFFECT

To verify the correlation between the ASMR triggering effect of an audio and its acoustic features, we conducted behavioral experiments on human participants using online questionnaire survey. U.S. participants were recruited from Amazon Mechanical Turk (MTurk) for remuneration. After providing informed consent, participants were asked to listen to 13 audio clips including 1 white noise and 12 ASMR audios, each lasting 10 s. The play order was independently and randomly shuffled for every participant to exclude the individual difference in repeated measurements. After listening to

TABLE II: Features extracted from synthesized ASMR audio clips

Audio Clip	Φ_1	Φ_2	Φ_3	Φ_4	Φ_5	Φ_6	Φ_7	Φ_8
Synthesized 1	4,70E-03	1,96E-06	0.1390	7,52E-05	7,82E-10	0.1250	2,39E-03	0.9580
Synthesized 2	1,09E-02	1,20E-05	0.1580	1,69E-04	4,18E-09	0.1100	2,86E-03	0.9500
Synthesized 3	1,58E-02	3,27E-05	0.1410	1,76E-04	9,65E-09	0.1400	1,40E-03	0.9335
Synthesized 4	5,09E-03	2,10E-06	0.1310	9,30E-05	1,18E-09	0.1240	1,72E-03	0.9622
Synthesized 5	3,73E-02	1,81E-04	0.1335	4,83E-04	7,99E-08	0.1231	1,36E-03	0.9866
Synthesized 6	1,07E-03	1,17E-07	0.1295	2,58E-05	9,30E-11	0.1073	4,09E-03	0.9455
Synthesized 7	7,71E-03	9,30E-06	0.1305	1,36E-04	4,89E-09	0.1139	7,76E-04	0.9769
Synthesized 8	9,66E-03	8,99E-06	0.1264	2,47E-04	1,00E-08	0.1066	1,02E-03	0.9634
Synthesized 9	2,14E-03	5,15E-07	0.1274	3,95E-05	3,68E-10	0.1144	1,11E-03	0.9776
Synthesized 10	7,30E-03	5,50E-06	0.1397	1,41E-04	3,81E-09	0.1090	7,99E-04	0.9584
Synthesized 11	4,96E-04	2,32E-08	0.1245	1,28E-05	4,00E-11	0.1151	2,05E-03	0.9558
Synthesized 12	1,17E-03	1,01E-07	0.1397	3,99E-05	2,08E-10	0.1140	1,25E-03	0.9696

TABLE III: Highlights of the perception scores and linear regression

Perceived Feeling	Average of 12 Recorded Clips			Average of 12 Synthesized Clips		
	Mean Score	Std. Deviation	Log-Likelihood	Mean Score	Std. Deviation	Log-Likelihood
<i>Negative</i>	1.6244	0.7302	-3028.8	1.5827	0.6353	-2874.2
<i>Positive</i>	1.5527	0.9109	-2703.8	1.2521	0.3605	-1695.0
<i>Relaxed</i>	1.6489	0.9953	-3468.6	1.3924	0.5093	-2695.7
<i>Attentive</i>	2.4112	1.6582	-3656.8	2.0072	1.1980	-3113.2
<i>General exp.</i>	0.6552	0.7727	-3529.8	0.5093	0.6232	-3035.2

TABLE IV: p -values by fitting the perception score of *relaxed* feelings

Fixed Variable	Φ_1	Φ_2	Φ_3	Φ_4	Φ_5	Φ_6	Φ_7	Φ_8
p -Value (recorded)	< 0.001	< 0.001	0.713	< 0.001	0.054	< 0.001	0.0800	0.145
p -Value (synthesized)	< 0.001	< 0.001	< 0.001	< 0.001	0.945	< 0.001	< 0.001	0.019

each audio clip, the participants reported their emotional state on 10 dimensions, namely *i*) nervous, *ii*) irritable *iii*) upset, *iv*) delighted, *v*) excited, *vi*) inspired, *vii*) attentive, *viii*) concentrating, *ix*) sleepy, and *x*) relaxed, which are selected from the widely-used PANAS scales [20]. Participants reported their emotions on 5-points scales (1 = “not at all”; 5 = “extremely”). In addition, participants were also asked about their *general experience* whether an ASMR effect had been triggered by the clip on a 3-point scale (0 = “no”; 1 = “no ASMR but a precursory ASMR-conductive state”; 2 = “yes”). For every completed survey, we took the average score of the emotions (*i-iii*) as the score for perception of *negative* feelings, and similarly the averages of (*iv-vi*), (*vii-viii*), (*ix-x*) for *positive*, *attentive*, and *relaxed* feelings, respectively. Thus, a 5D-vector of perception score was obtained from each survey.

The experiment was conducted twice, first with 249 participants using the recorded ASMR audio clips in Tab. I, and the second with 251 participants using the synthesized clips in Tab. II. After each experiment, we carried out regression analysis on the collected set of scores w.r.t. the acoustic features Φ_1 - Φ_8 , using the linear mixed-effect model (LMM):

$$y = \beta_0 + \sum_{i=1}^8 \beta_i \Phi_i + \sum_{i=0}^8 b_i z_i + \epsilon, \quad (4)$$

where y can be used to fit every dimension of the perception score vector. ϵ is the model error, β_0 the constant offset, β_1 - β_8 the linear coefficients regarding features Φ_1 - Φ_8 , respectively. The random variables z_1 - z_8 weighted by coefficients b_1 - b_8 are introduced to capture the random effect caused by repeated measures, which is suggested as a standard approach in cognitive neuroscience and experimental psychology [21].

Some statistics of the score data and model fitting results are highlighted in Tab. III. Compared with the recorded clips, our synthesized audio clips are performing similarly in triggering emotional perceptions and ASMR experiences, with a slightly enhanced suppression of negative emotions, but weaker effect in other perspectives. The low likelihood of model implies that the perception scores are *very unlikely* linear functions of the extracted acoustic features, which is not surprising due to the high non-linearity of human neural systems and cognition processes. Nevertheless, we can surely affirm a significant correlation between the ASMR triggering effect and the acoustic features, with the extremely low p -values as supporting evidence (e.g. Tab. IV for *relaxed* feelings).

VI. CONCLUSION AND OUTLOOKS

In this paper, we have studied the phenomenon of ASMR from an acoustic perspective, and successfully affirmed a significant correlation between the ASMR triggering effect and the cyclic spectral characteristics of audios. Crucially, we have implemented a DCGAN-based system, which synthesizes random artificial audio clips that can effectively trigger ASMR.

For future research, two approaches can be potentially interesting. From the signal processing and AI perspective, a novel application-specific design of DCGAN that directly generates audio waveform without relying on spectrogram images may help further improve the quality and ASMR triggering effect of the synthesized audios. From the psychological perspective, replacing the behavioral study with neuroimaging techniques may help us better observe the ASMR effect and understand the psychological mechanism behind it.

REFERENCES

- [1] E. L. Barratt and N. J. Davis, "Autonomous Sensory Meridian Response (ASMR): A flow-like mental state," *PeerJ*, vol. 2015, p. e851, 3 2015. [Online]. Available: <https://peerj.com/articles/851>
- [2] P. C. Harper, "ASMR: Bodily pleasure, online performance, digital modality," *Sound Studies*, vol. 6, pp. 95–98, 2019. [Online]. Available: <https://www.tandfonline.com/doi/abs/10.1080/20551940.2019.1681574>
- [3] C. Spence, Q. J. Wang, F. Reinoso-Carvalho, and S. Keller, "Commercializing sonic seasoning in multisensory offline experiential events and online tasting experiences," *Frontiers in Psychology*, vol. 12, p. 4150, 9 2021.
- [4] G. L. Poerio, E. Blakey, T. J. Hostler, and T. Veltri, "More than a feeling: Autonomous sensory meridian response (ASMR) is characterized by reliable changes in affect and physiology," *PLOS ONE*, vol. 13, p. e0196645, 6 2018. [Online]. Available: <https://journals.plos.org/plosone/article?id=10.1371/journal.pone.0196645>
- [5] B. C. Lochte, S. A. Guillory, C. A. Richard, and W. M. Kelley, "An fMRI investigation of the neural correlates underlying the autonomous sensory meridian response (ASMR)," *BioImpacts : BI*, vol. 8, p. 295, 2018. [Online]. Available: <https://pubmed.ncbi.nlm.nih.gov/31209833/>
- [6] E. L. Barratt, C. Spence, and N. J. Davis, "Sensory determinants of the autonomous sensory meridian response (ASMR): Understanding the triggers," *PeerJ*, vol. 2017, p. e3846, 10 2017. [Online]. Available: <https://peerj.com/articles/3846>
- [7] G. G. Cole and A. J. Wilkins, "Fear of holes," *Psychological Science*, vol. 24, pp. 1980–1985, 8 2013. [Online]. Available: <https://journals.sagepub.com/doi/full/10.1177/0956797613484937>
- [8] W. A. Gardner, A. Napolitano, and L. Paura, "Cyclostationarity: Half a century of research," *Signal processing*, vol. 86, no. 4, pp. 639–697, 2006.
- [9] I. J. Goodfellow, J. Pouget-Abadie, M. Mirza, B. Xu, D. Warde-Farley, S. Ozair, A. Courville, and Y. Bengio, "Generative adversarial networks," *arXiv preprint arXiv:1406.2661*, 2014.
- [10] I. Goodfellow, J. Pouget-Abadie, M. Mirza, B. Xu, D. Warde-Farley, S. Ozair, A. Courville, and Y. Bengio, "Generative adversarial networks," *Communications of the ACM*, vol. 63, no. 11, pp. 139–144, 2020.
- [11] H.-W. Dong, W.-Y. Hsiao, L.-C. Yang, and Y.-H. Yang, "MuseGAN: Multi-track sequential generative adversarial networks for symbolic music generation and accompaniment," in *Proceedings of the AAAI Conference on Artificial Intelligence*, vol. 32, no. 1, 2018.
- [12] S. Lee, B. Ko, K. Lee, I.-C. Yoo, and D. Yook, "Many-to-many voice conversion using conditional cycle-consistent adversarial networks," in *ICASSP 2020 - 2020 IEEE International Conference on Acoustics, Speech and Signal Processing (ICASSP)*, 2020, pp. 6279–6283.
- [13] K.-W. Kim, S.-W. Park, J. Lee, and M.-C. Joe, "ASSEM-VC: Realistic voice conversion by assembling modern speech synthesis techniques," in *ICASSP 2022 - 2022 IEEE International Conference on Acoustics, Speech and Signal Processing (ICASSP)*, 2022, pp. 6997–7001.
- [14] L. N. Ferreira, L. Mou, J. Whitehead, and L. H. Lelis, "Controlling perceived emotion in symbolic music generation with monte carlo tree search," in *Proceedings of the AAAI Conference on Artificial Intelligence and Interactive Digital Entertainment*, vol. 18, no. 1, 2022, pp. 163–170.
- [15] A. Radford, L. Metz, and S. Chintala, "Unsupervised representation learning with deep convolutional generative adversarial networks," in *4th International Conference on Learning Representations, ICLR 2016, San Juan, Puerto Rico, May 2-4, 2016, Conference Track Proceedings*, 2016.
- [16] S. Ioffe and C. Szegedy, "Batch normalization: Accelerating deep network training by reducing internal covariate shift," in *International conference on machine learning*. PMLR, 2015, pp. 448–456.
- [17] A. Gautam, M. Sit, and I. Demir, "Realistic river image synthesis using deep generative adversarial networks," *arXiv preprint arXiv:2003.00826*, 2020.
- [18] D. P. Kingma and J. Ba, "Adam: A method for stochastic optimization," *arXiv preprint arXiv:1412.6980*, 2014.
- [19] I. Bayram, "An analytic wavelet transform with a flexible time-frequency covering," *IEEE Transactions on Signal Processing*, vol. 61, no. 5, pp. 1131–1142, 2012.
- [20] D. Watson, L. A. Clark, and A. Tellegen, "Development and validation of brief measures of positive and negative affect: The PANAS scales." *Journal of personality and social psychology*, vol. 54, no. 6, p. 1063, 1988.
- [21] D. A. Magezi, "Linear mixed-effects models for within-participant psychology experiments: an introductory tutorial and free, graphical user interface (LMMgui)," *Frontiers in psychology*, vol. 6, p. 2, 2015.